LUND UNIVERSITY
Faculty of Science

Mathematically modelling the coaction of cancer radiotherapy and immunotherapy

Arthur Simbarashe Chakwizira

Thesis submitted for the degree of Bachelor of Science
Project duration: 5 months

Supervised by Crister Ceberg and Kristina Stenström

Department of Medical Radiation Physics
Department of Physics
May 2017

List of abbreviations and acronyms

1-MT	1-methyltryptophan
ARG	Arginase
CTL	Cytotoxic T-lymphocyte
CTLA-4	Cytotoxic T-lymphocyte-associated protein 4
DNA	Deoxyribonucleic acid
IDO	Indoleamine 2,3-dioxygenase
IL-10	Interleukin 10
MDSC	Myeloid-derived suppressor cell
NK	Natural killer
NO	Nitric oxide
PD-1	Programmed cell death protein 1
PD-L1	Programmed death-ligand 1
ROS	Reactive oxygen species
T_{reg}	Regulatory T-cell
TAM	Tumour-associated macrophage
TGF-β	Transforming growth factor - beta

Contents

Acknowledgements

I would like to thank my supervisors Crister Ceberg and Kristina Stenström for their invaluable support during the thesis project. I am truly grateful for the inspiring talks I had with Crister, without whom this project would not have been possible. Kristina provided wholehearted assistance, especially with the report writing. Thank you.

1 Introduction

Cancer, despite medical advancements made to curb its fatality, is still among the leading causes of death [1]. Its incidence is projected to nearly double in the next twenty years [1]. In order to diminish cancer-related mortality, it is imperative that cancer treatment methods with higher efficacy are developed.

What makes cancer a challenge to treat, let alone cure, is the fact that, unlike common diseases, it has the ability to both evade and suppress the body's native defense system - the immune system [2]. Traditionally, cancer treatment has been administered following one of three modalities: radiation, chemotherapy and surgery [2].These therapies, and their combinations, do not always suffice especially when one considers cancers such as glioblastoma (the deadliest and most prevalent of brain tumours in adults [3]). Radiation is known to affect the patient's immune system in either a stimulatory or detrimental manner, depending on the dose. There is growing innovation towards exploiting the immunostimulatory effect of radiation by combining it with immunotherapy (the administration of drugs that prevent the tumour from escaping the immune system) [4]. In combining the two treatment strategies, it is crucial to consider not only the radiation dose, but also the dose fractionation (scheduling). Determining the optimal dose regimen is made a formidable task by the sheer number of variables that have to be taken into account. Were the optimisation to be done through trial and error in *in vivo* experiments, it would require an unrealistic number of samples to study the effects of varying the numerous parameters. Convenient would be a mathematical model which could function as a basis for computer simulations. This would enable the performance of a large number of *in silico* experiments, the results of which could form a framework for actual experiments. To this end, this project focused on a study of the coaction of cancer radiotherapy and immunotherapy using two mathematical models adapted from the papers by Serre et al. [6] and Wilkie and Hahnfeldt [7].

1.1 Radiotherapy

Radiotherapy is the application of ionising radiation to locally destroy, or hinder the growth of, a cancer tumour. Ionising radiation induces the liberation of one or more electrons from atoms of the medium it traverses [10]. The radiation may be either a high-energy (1 MeV - 25 MeV [8]) beam of X- or γ-rays or particulate radiation (electrons, protons, etc) [16]. X-rays are produced as brehmsstrahlung radiation upon the deceleration of high-speed electrons by a metal target. The radiation is then filtered to produce a beam suitable for clinical applications. Gamma rays originate from excited nuclei of radioactive isotopes de-exciting to their ground states [16].

1.1.1 Photon interactions

The particle-like nature of electomagnetic radiation manifests itself in the form of photons [9]. Photons are massless particles of zero charge that travel at the speed of light. Upon incidence on matter, they can either penetrate without interacting, be completely absorbed by the target material or scatter from the material losing part of their energy in the process. As opposed to charged particles that deposit energy through Coulombic interactions with electrons of the target material, photons lose energy following one or more of three modes: the photoelectic effect, Compton scattering or pair production [9].

Photoelectic effect
In the photoelectic effect, the incoming photon transfers its energy to an electron in one of the bound energy levels of the target atom and completely vanishes [9]. This electron (a photoelectron) leaves the atom with a kinetic energy E_k given by

$$E_k = hf - E_b \tag{1.1}$$

where h is Planck's constant, f is the frequency of the incident photon (thus hf is its energy) and E_b is the binding energy of the photoelectron. Which energy level the photoelectron emerges from depends on the energy of the photon. For gamma rays of sufficient energy, the photoelectron most likely comes from the K-shell, the most tightly bound energy level. Regimes in which the photoelectic effect dominates are low photon energies and high atomic numbers (Z). The probability of photoelectic absorption (τ) is given by

$$\tau = \frac{Z^n}{(hf)^3} \tag{1.2}$$

where Z, h and f are as defined earlier and n varies between 3 and 4. The strong dependence of the probability of the photoelectic effect on Z implies that this energy loss channel is not pronounced in soft tissue which is dominated by low Z material [9].

Compton scattering
In Compton scattering, the incident photon is deflected by an electron of the absorbing material through an angle. In the process, the photon transfers a fraction of its energy to the electron. The energy given to the electron can take any value from zero to a large portion of the original photon energy. Compton scattering is the most dominant energy loss channel in soft tissue for photon energies ranging from 100 keV to 10 MeV [9]. The probability of Compton scattering is almost independent of atomic number, inversely proportional to photon energy and directly proportional to the number of electrons per gram (which varies by 20% from the heaviest to the lightest elements) [9].

Pair production
For photons of energies above 1.022 MeV (twice the rest energy of an electron), pair production is a possible energy loss mechanism [9] . This occurs when the photon, traversing the vicinity of a target nucleus, experiences strong field effects that induce its annihilation into an electron-positron pair. The pair emerges with kinetic energies given by

$$E_{e+} + E_{e-} = hf - 1.022 \text{ (MeV)} \tag{1.3}$$

where E_{e+} and E_{e-} are the kinetic energies of the positron and electron, respectively and hf is the energy of the incident photon. The probability of pair production is proportional to the photon energy and to the square of the atomic number [9].

1.1.2 Radiometry and dosimetry

This section provides definitions of some important radiometric and dosimetric quantities. Radiometric quantities are used to mathematically characterise the radiation field [10]. They are related to either the number of particles in the radiation field (N) or the energy they transfer (radiant energy, R). If N particles have energy E (which excludes the rest energy), their radiant energy is given by $R = NE$. The distributions of N and R with respect to energy are given respectively by $N_E = dN/dE$ and $R_E = dR/dE$ where dN is the number of particles with energies in the range $[E, E + dE]$ and dR is the corresponding radiant energy. By analogy, the following holds: $R_E = EN_E$. Dosimetric quantities concern the interaction of ionising radiation with organic tissue.

Particle fluence
Particle fluence, ϕ is the number of incident particles on a sphere of cross-sectional area a and is given by

$$\phi = \frac{dN}{da} \tag{1.4}$$

where da is measured perpendicular to the direction of motion of each particle [10].

Cross section
Cross section, σ, is defined by

$$\sigma = \frac{N}{\phi} \tag{1.5}$$

where N is the average number of target interactions with particles that have a fluence ϕ. In the case in which the incident particles interact with the target distinctly and independently, the total cross section is the sum of the individual cross sections:
$\sigma = \sum \sigma_j = \frac{1}{\phi} \sum N_j$ with N_j being the mean number of interactions with particles of type j [10].

Mass attenuation coefficient
The mass attenuation coefficient, μ_m, of a material upon interaction with uncharged particles of a certain type and energy is given by

$$\mu_m = \frac{\mu}{\rho} = \frac{1}{\rho dl}\frac{dN}{N} \tag{1.6}$$

where ρ is the density of the material, μ is the linear attenuation coefficient, $\frac{dN}{N}$ is the mean fraction of particles that undergoes interaction when traversing a length dl of material. It is related to the total cross section, σ, through $\mu_m = \sigma \times N_A/M$ where N_A is Avogadros constant and M is the molar mass of the target material [10]. The mass attenuation coefficient is preferred because it eliminates the dependence on density that is exhibited by the linear attenuation coefficient [10]. It is important to note that the linear attenuation coefficient gives the probability of an interaction per unit distance traveled [9]. This coefficient also depends on the energy of the interacting photon [9].

Linear energy transfer
The linear energy transfer, L_Δ, of a material upon interaction with charged particles of a certain type and energy is given by

$$L_\Delta = \frac{dE_\Delta}{dl} \tag{1.7}$$

where dE_Δ is the mean energy deposited by the charged particles traversing a distance dl in the material [10]. This excludes the mean sum of the kinetic energies larger than Δ of electrons released by the charged particles. Δ is thus an energy cutoff.

Energy deposit
Energy deposit, ϵ_i, is the energy deposited per interaction and is given by

$$\epsilon_i = \epsilon_{in} - \epsilon_{out} + Q \tag{1.8}$$

where ϵ_{in} is the energy of the incident ionising particle and ϵ_{out} is the sum of the energies of all ionising particles (disregarding charge) emerging from the interaction [10]. Both ϵ_{in} and ϵ_{out} exclude the rest energies of the particles. Q is the change in rest energy of the nucleus and of all elementary particles involved in the interaction [10].

Energy imparted
Energy imparted, ϵ, is the total of all energy deposits in a given volume of matter [10]. It is defined as

$$\epsilon = \sum_i \epsilon_i \tag{1.9}$$

The summation is performed over one or more energy-deposition events (particle trajectories). The mean energy imparted $\bar{\epsilon}$ is given by

$$\bar{\epsilon} = R_{in} - R_{out} + \sum Q \tag{1.10}$$

where R_{in} and R_{out} are the mean radiant energies of all ionising particles entering and leaving a given volume of matter, respectively [10]. Q is the change in rest energy of all nuclei and elementary particles present in the volume.

Specific energy
The specific energy is the energy imparted per unit mass by ionising radiation in a volume of matter, and is given by

$$z = \frac{\epsilon}{m} \tag{1.11}$$

where z is the specific energy, ϵ is the imparted energy and m is the mass of the material in the volume [10].

Absorbed dose
The absorbed dose, D, is the mean energy imparted by ionising radiation per unit mass. It is given by

$$D = \frac{d\bar{\epsilon}}{dm} \tag{1.12}$$

where $\bar{\epsilon}$ is the mean energy imparted and m is the mass of the target volume of matter [10]. The SI unit of D is Jkg^{-1} but it is given the name Gray (Gy). It is important to note that the specific energy, z, is a stochastic quantity. Numerous measurements of z would produce a probability distribution of z values and a mean $\bar{z}$, which is the absorbed dose D. Knowledge of the distribution of z for a known D is important since for small masses (such as in cells), the effect of radiation is more accurately described by z than by D [10].

1.1.3 Radiobiological action

The probability of survival of a cell exposed to radiation can be described by the hit and target model [11]. The DNA molecule is the target of radiation. When it is hit by ionising radiation, a DNA strand break occurs, causing a failure in the transfer of genetic information and consequent loss of the cell's ability to grow. DNA strand breaks result from either direct action where the radiation directly interacts with the DNA molecule producing a lesion, or from indirect action where the damage results from a secondary process.

Direct action

Every cell has a critical target (DNA) whose destruction leads to the death of the cell [11]. Whether an irradiation event is fatal or not depends on the number of radiation particles hitting the critical target. The probability, P_{hit} that exactly j such particles interact with the target is given by the binomial distribution:

$$P_{hit}(j) = \binom{Dx}{j} p^j (1-p)^{Dx-j}, j = 0, 1, 2, ..., Dx \tag{1.13}$$

where D is the radiation dose, x is the number of particles per unit dose and p is the (constant) probability that a radiation particle will hit the critical target. Assuming a Poisson distribution of lesions, letting $Dx \to \infty$ and setting $Dxp = \lambda D$ (where λ is a parameter relating to the radiosensitivity of the target cell), equation 1.13 becomes

$$P_{hit} = \frac{(\lambda D)^j}{j!} e^{-\lambda D} \tag{1.14}$$

The probability that the cell dies is then given by

$$P_{death} = \sum_{j=k+1}^{\infty} \frac{(\lambda D)^j}{j!} e^{-\lambda D}, k = 0, 1, 2, ... \tag{1.15}$$

where k is the critical number of radiation-induced primary lesions that the cell can survive. The probability of survival of the cell is then given by

$$P_{surv}(D) = \sum_{k=0}^{\infty} e^{-\lambda D} \phi(k) \sum_{j=0}^{k} \frac{(\lambda D)^j}{j!} \tag{1.16}$$

where ϕ is a function satisfying $\phi(j) \geq 0 \ \forall j$ and $\sum_j \phi(j) = 1$ [11].

Indirect action

Radiation can also be absorbed by neighbouring water molecules, causing the generation of highly reactive free radicals (atoms bearing an unpaired valence electron) [11]. These radicals react with and modify DNA, causing biological damage. The process by which free radicals are formed from water molecules begins with the ionisation of water (radiolysis) according to the chemical equation

$$\mathrm{H_2O} \longrightarrow \mathrm{H_2O^{+*}} + \mathrm{e^{-*}} \tag{1.17}$$

where "*" represents a state of excitation. The unstable water ion $\mathrm{H_2O^{+*}}$ de-excites via the following reaction

$$\mathrm{H_2O^{+*}} + \mathrm{H_2O} \longrightarrow \mathrm{H_3O^+} + \cdot\mathrm{OH} \tag{1.18}$$

where ·OH is a free radical formed from the loss of one electron from the hydroxyl ion (OH^-). This electron collides with neighbouring water molecules, loses energy and eventually becomes a hydrated electron, according to

$$e^{-*} \longrightarrow e^-; \qquad e^- + nH_2O \longrightarrow e^-_{aq} \tag{1.19}$$

where n is a positive integer and the subscript aq represents an aqueous state [11]. The excited water molecule from equation 1.18 de-excites by the formation of more toxic hydroxyl radicals according to

$$H_2O^* \longrightarrow H\cdot + \cdot OH \tag{1.20}$$

Survival probabilities
DNA damage can occur in the form of double strand or single strand breaks [11]. Several models can be used to describe the survival probability of an irradiated cell, taking into account DNA repair. The most widely used is the linear-quadratic (LQ) model. The LQ model considers both single and double strand breaks, and also assumes that the former is easier to repair than the latter. The biological effect of radiation is based on a linear term and a quadratic term. Cell death results from single lethal hits and accumulated damage from two independent sublethal hits [12]. The combined effect results in a cell survival probability, S, given by the equation

$$S(D) = e^{-(\alpha D + \beta D^2)} \tag{1.21}$$

where α and β represent the formation of a double strand break by one and by two radiation particles, respectively and D is the radiation dose. The sensitivity of tissue to fractionated radiation can be characterised by the α/β ratio and for tumours, good agreement has been observed when this ratio is larger or equal to 10 Gy [11]. α/β corresponds to the dose at which damage from single hits equals damage from accumulated sublethal lesions [12].

1.1.4 Clinical impact of the linear-quadratic model

Irradiation of tumours is conventionally done using small daily doses of 2 Gy per fraction over a period of about 6 weeks [12]. The goal is to increase radiation dose to the tumour while preventing harm to normal tissue. The LQ model is used by over 90% of radiation oncologists to predict the effect of radiation on cells and clinical studies fit predictions of the model relatively well [12]. The model has, however, shortcomings. Both α and β vary with cell cyle (the stage of growth at which a cell is). The model is most reliable for doses in the range $(1-6)$ Gy and loses accuracy outside of this range (at high doses, D^2 dominates the equation 1.21). Furthermore, the model assumes uniform effect per

radiation fraction. The response to fractionation varies with tissue: some tissues are acute-responding while others are late-responding. Heterogeneity within and between tumours results in large uncertainties in the α/β values [12]. In addition, the LQ model does not account for other cell populations or factors in the tumour microenvironment. Therefore, more elaborate models are needed when combining radiotherapy and other therapies.

1.1.5 Tumour growth models

Despite complex internal interactions, tumour growth kinetics follow fairly simple patterns that can be described by mathematical models [13]. All the models described in this section consider the variation of the total tumour volume, V, with time, t. V is assumed to be proportional to the number of cells in the tumour. All the models assume $V(t=0) = V_0$ [13].

Exponential-linear models
All cells are assumed to grow with a constant cell cycle duration T_C, leading to exponential growth [13]. The initial exponential growth stage is assumed to preceed a linear growth phase. The following Cauchy problem describes the system

$$\begin{cases} \frac{dV}{dt} = a_0 V, & t \leq \tau \\ \frac{dV}{dt} = a_1, & t > \tau \\ V(t=0) = V_0 \end{cases} \tag{1.22}$$

where $a_0 = (\ln 2/T_C \times$ fraction of proliferative cells), a_1 is the slope in the linear growth phase and τ is the time point at which the linear growth commences.

Logistic and Gompertz models
These models describe tumour growth characterised by a sigmoid curve (a monotonously increasing curve with one inflection point beyond which the curve asymptotically approaches a maximum volume, which is the carrying capacity) [13]. The logistic growth model is described by

$$\frac{dV}{dt} = aV\left(1 - \frac{V}{K}\right); \qquad V(t=0) = V_0 \tag{1.23}$$

where a is a constant related to growth kinetics and K is the tumour carrying capacity. In other cases, the generalised logistic growth model is adapted instead. This is defined by

$$\frac{dV}{dt} = aV\left(1 - \left(\frac{V}{K}\right)^v\right); \qquad V(t=0) = V_0 \tag{1.24}$$

where v is an adjustable parameter. Replacing a by $\beta = \frac{a}{v}$ and allowing $v \to 0$, the generalised logistic growth model converges to the Gompertz model described by

$$\frac{dV}{dt} = ae^{-\beta t}V; \qquad V(t=0) = V_0 \tag{1.25}$$

where a is the rate of initial proliferation (at $V = V_0$) and β is the rate of exponential decay of a.

Some models unite the ones described above [14] while others consider a dynamic carrying capacity as opposed to the constant one used so far [15]. These models describe unperturbed tumour growth and therefore do not take into account either the existence of other cells (such as immune cells) in the tumour microenvironment or the effect of external influences (such as radiation or other kinds of therapy). More comprehensive and adapted models are needed for describing tumour growth in an environment influenced by the mentioned factors. As noted in the beginning of this text, two such models were considered in this work, and descriptions of both are provided in later sections.

1.2 Immunotherapy

Cancer immunotherapy is a treatment modality that summons the immune system to eliminate tumour cells (primary immune response) and/or prevent their future occurrence (secondary immune response) [6].

The immune system employs a system of checkpoints to distinguish normal cells from aberrant or foreign ones. These checkpoints are controlled by inhibitors, which are molecules (such as PD-1) on the surfaces of certain immune cells. If PD-1 binds with the ligand PD-L1 found on normal cells (and some tumour cells), it directs the immune system to leave the PD-L1-bearing cell alone [6]. Another system of checkpoint inhibitors is the CTLA-4 pathway, which prevents the proliferation of premature immune cells that may react to healthy cells in the early stages of activation [19]. Cancer cells exploit such inhibitors to evade the immune system as part of a process called immunoediting [2]. In the early stages of tumour development, there is an active anti-tumour immune response. However, over time, the tumour expresses healthy-cell signals to lure away the immune system and therefore modulate the immune response [2].

Consider Figure 1 which illustrates the features responsible for the low immunogenicity (quality of being recognisable by the immune system [6]) of the cancer tumour. The primary mechanism by which the tumour microenvironment evades immune surveillence is the emission of cytokines, substances released by particular cells of the immune system that affect other cells. T_{reg}s emit the proteins TGF-β and IL-10 while MDSCs release NO, ROS and ARG. Regulatory dendritic cells emit IL-10 and IDO, whereas TAMs emit ARG and TGF-β to counteract the effect of NK cells. The overall effect of these cytokines is to modulate the killing function of CTLs. Figure 1 also shows that the tumour can express the ligands FasL and PD-L1. The combination of the FasL ligand with the Fas receptor

on the surface of a CTL will directly induce T-cell apoptosis (death). FasL and TGF-β may also be produced by host cells such as endothelial cells and fribroblast [18].

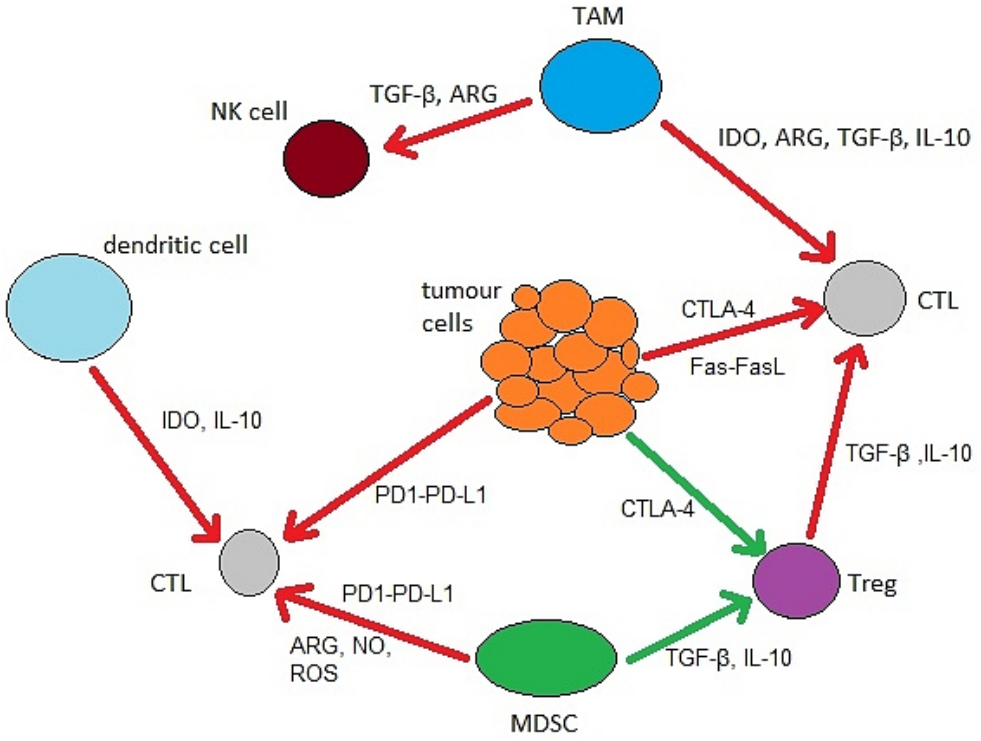

Figure 1: Characterisitcs of the tumour microenvironment that enable evasion and suppression of the immune system (immunoediting). The tumour secretes the labeled cytokines to modulate the effect of immune cells (CTLs and NK cells). Green arrows represent a relationship of activation while red ones signify inhibition. [18]

Immunotherapy may take the form of immune checkpoint blockade, where the mentioned inhibitory pathways (CTLA-4 and PD-1-PD-L1) that would normally reduce the activity of immune cells, are interrupted. Drugs that have been approved and are in clinical use include Ipilimumab (CTLA-4) and Nivomulab and Pembrolizumab (PD-1-PD-L1) [18].

Alternatively, drugs that inhibit the expression of IDO may be administered. IDO induces the activation of T_{reg}s (cells that interfere with the action of immune cells) and their introduction into the tumour microenvironment. It is also an enyzyme catalysing the oxidation of tryptophan, a substance whose dimunition inhibits immune cells. An appropriate drug that counteracts IDO activity and has been approved for clinical trials is 1-MT. It is especially applied to the treatment of glioblastoma [20]. Nevertheless, on its own, immunotherapy fails to reverse the process of cancer immunoediting [2].

1.3 Radiotherapy and Immunotherapy

As noted earlier, radiation is traditionally administered in small daily doses of 2 Gy until a high total dose of 60 -70 Gy is attained. However, studies reveal that single-fraction radiation can enhance the effect of the immune system by destroying immune-repressive cells such as T_{reg}s, macrophages and MDSCs [21]. Section 1.1 highlighted that radiation primarily leads to tumour cell death. It can, however, also enhance an anti-tumour immune response through inducing the release of tumour antigens (danger-associated proteins that trigger an immune response). These effects are dependent on the fractionation scheme used to supply the radiation. It has been shown that, as opposed to the conventional multi-fraction irradiation regimen, supplying a single dose of radiation will cause a notable increase in the population of tumour-associated antigens [2]. This will in turn trigger the activation and recruitment of immune cells, provided they are not terminated by subsequent doses [21]. Note should me made, nonetheless, that radiation also damages healthy cells in the vicinity of the tumour, but these can usually repair themselves, provided the absorbed dose is below their tolerance limit [16]. Radiation can thus revitalise the immune system to exercise control over the tumour. This interplay is the backbone of the combination therapy explored in this project. Key is to determine the best radiation dosage scheme to employ so that the immunogenicity of the tumour is increased simultaneously as the activated, recruited immune cells are kept un-irradiated.

2 Materials and Methods

As mentioned in the introduction, the investigation in this thesis work was based on two mathematical models adapted from Wilkie and Hahnfeldt [7] and from Serre et al [6], which may be coined the Wilkie and Serre models, respectively. The Wilkie model, originally adapted to modelling cancer treatment with immunotherapy alone, offers a description of the interaction of a cancer tumour with the host immune system. It incorporates the phenomenae of immune-predation and immune-recruitment to modify the generalised logistic growth of an undisturbed tumour. The Serre model encompasses the temporal dynamics of the tumour, tumour antigens, lymphocytes (immune cells) as well as the primary and secondary immune responses. A description of both models and how they were implemented in MATLAB is provided in this section.

As alluded to earlier, this area of study is relatively new. Prior to this project, only one experiment and publication had been done on combination therapy involving single-fraction radiation and 1-MT [20]. For that reason, it was instructive to carry out investigations using two models, since a result confirmed by two independent models is necessarily more credible than one deduced from a single one. The primary purpose of the Wilkie model was to verify that there does exist a synergy between radiotherapy and immunotherapy, and that the success of this combination therapy depends largely

on the radiation dose fractionation. For that reason, the Wilkie model was not fitted to the experimental data that were availabe at the Medical Radiation Physics department (glioblastoma data from Ahlstedt et al. [20] and Ceberg et al. [24]), but was instead adapted with the parameters estimated by Wilkie and Hahnfeldt [7]. Given how numerous the parameters in the model were, keeping the ones deduced during the derivation of the model also ensured a narrower margin of error.

Having with the Wilkie model established the presence of a synergy between radiotherapy and immunotherapy as well as the importance of fractionation, the Serre model was then used to determine the actual dose and fractionation that would lead to highest treatment efficacy. It was thus necessary to fit this model to actual experimental data.

2.1 Wilkie model

The Wilkie model describes the evolution of tumour cells in an immune-cell-infiltrated environment. Interactions that are taken into account are the predation of the cancer cells by immune cells and the recruitment of immune cells by cancer cells. Cancer-mediated recruitment of immune cells occurs via the secretion of danger-associated molecules such as antigens. Key to the foundation of the model is that the interaction of the tumour and immune system culminates in a dormant tumour state characterised by the cessation of mitosis (cell division, tumour growth). Depending on whether conditions favour tumour proliferation or regression, this dormant state will progress into tumour escape or elimination. An analogy can be recongnised between this description and the concept of immunoediting descibed in Section 1.2. Both the tumour and the immune cell populations grow up to an equilibrium phase where, if immunoediting is not hampered, the tumour flourishes irreversibly. In this model, both the immune cell and cancer cell populations are assumed to exhibit generalised logistic growths (see Section 1.1.5).

2.1.1 Cancer cell population

The time-variation of the cancer cell population is given by

$$\frac{dC}{dt} = \frac{\mu}{\alpha}\Big(1 + \Psi(I, C)\Big)C\bigg(1 - \bigg(\frac{C}{K_C}\bigg)^{\alpha}\bigg); \qquad C(0) = C_0 \tag{2.26}$$

$C(t)$ is a measure of the tumour cell population at time t. μ and α are constants related to the growth rate of the tumour and its sensitivity to environmental growth regularoty signals. $\Psi(I, C)$ is the immune predation factor, which models the cytotoxic effect of immune cells against cancer cells. It is necessarily negative so as to hinder tumour advancement. The factor K_C is the tumour carrying capacity, which is the maximum tolerable tumour cell population. In the absence of immune predation, the tumour will grow to this size and the organism will perish. C_0 is the initial number of tumour cells, that is, the number of cancer cells introduced into the organism at the time of innoculation. The cancer cell

population is, in accordance with the earlier discussion, modulated by immune predation. It also depends on the present number of cancer cells, since this controls the quantity of antigens released as well as the rate of growth of the tumour mass.

2.1.2 Immune cell population

The immune cell population is assumed to comprise CTLs and NK cells, which have a direct inhibitory effect on the tumour. The rate of change of the immune population is given by

$$\frac{dI}{dt} = \lambda(1 + rC)\left(1 - \frac{I}{K_I}\right); \qquad I(0) = I_0 \tag{2.27}$$

$I(t)$ is the immune cell population at time t and λ is the immune growth parameter. r is an immune recruitment factor and the product rC represents cancer-cell mediated immune recruitment. K_I is the immune carrying capacity and is analogous to K_C. The immune cell population does not grow indefinitely, it is modulated by the limit K_I. It should be noted that K_I is a theoretical limit. I_0 is the initial number of immune cells, which may be zero. In adherence to the presented theory, the immune population depends on the rate of immune recruitment, the number of present immune cells as well as the current cancer cell population.

2.1.3 Immune predation

The immune predation term is given by

$$\Psi(I, C) = -\theta\left(\frac{I^\beta}{\phi C^\beta + I^\beta} + \epsilon \log_{10}(1 + I)\right) \tag{2.28}$$

where $\Psi(0, 0) = 0$ by definition. The action of the immune system is divided into an innate and an adaptive component. Equation 2.28 above captures both effects. For small I, the ratio-dependent term dominates the equation and thus can be regarded as a composition of both the innate and adaptive parts of the immune response. However, for large I, the cytotoxic effect of the innate immune response has to be considered and this is described by the logarithmic term. This extra term is important because the ratio-dependent term alone leads to a saturation in the predation for large I, but saturation does not occur in the innate immunity. The logarithmic term (coupled with the constant epsilon) then allows for a gentle rise in the predation saturation limit for sharp increases in the immune cell population. θ is the predation strength and ϕ and β are constants related to predation saturation.

2.1.4 Implementation

As already mentioned, the Wilkie model was especially adapted to cancer treatment with immunotherapy. Radiation had to be introduced into the system using the linear-quadratic model, discussed in section 1.1.3. According to the theory presented in that section, the effect of radiation is to kill off a certain fraction of the tumour cells. This effect was captured by the probability of survival $S(d)$ of the tumour upon exposure to a radiation dose d. $S(d)$ was given by

$$S(d) = \mathrm{e}^{-\alpha_{rad} \cdot d - \beta_{rad} \cdot d^2} \tag{2.29}$$

where α_{rad} and β_{rad} are constants of the linear-quadratic model.

The differential equations 2.26 and 2.27 were solved numerically in MATLAB using a fourth-order Runge-Kutta routine (see Appendix C). The time unit (one day) was discretised in 100 time-steps and the integration was carried out over 120 days. Radiation was given over four time-steps, with a dose rate of 2 Gy per time-step, corresponding to a total dose of 8 Gy given over an hour per day. The radiation dose d was consequently treated as a vector of length $N, (N = 12000)$, with non-zero components in those time-steps where radiation was administered. The effect of irradiation was incorporated into the dynamics of the tumour population, C, in MATLAB as

$$C(q, n+1) = \min\left(C_{max}, S(d(n)) \cdot \left(C(q,n) + \frac{1}{6} \cdot (c_1 + 2c_2 + 2c_3 + c_4) \right) \right) \tag{2.30}$$

where $C(q,i), i \in N$, is the tumour population in the qth animal in time-step i, $c_k, k = 1,2,3,4$ are parameters of the Runge-Kutta routine in MATLAB , C_{max} is the maximum tumour population the organism is allowed to live with and $S(d(n))$ is the survival probability of tumour cells upon exposure to the radiation dose d given in time-step n.

Radiation, as noted in section 1.3, affects healthy cells in the same way it does cancer cells. Consequently, the effect of irradiation on the immune cells present in the tumour microenvironment at the time of irradiation had to be considered. It was assumed that radiation kills all of such cells with unit probability. Similar to the tumour-population case, radiation-induced immune-cell death was incorporated into the system as

$$I(q, n+1) = \delta(n) \cdot \left(I(q,n) + \frac{1}{6}(i_1 + 2i_2 + 2i_3 + i_4) \right) \tag{2.31}$$

where δ is a parameter that assumes the value zero in every time-step where the dose vector d has a non-zero component, and the value 1 otherwise. $I(q,i), i \in N$, is the immune population in the qth animal in time-step i and $i_k, k = 1,2,3,4$ are parameters of the Runge-Kutta routine in MATLAB.

In order to mimic a physical situation, in which cancer prognosis with or without treatment is non-uniform across individuals of a test group of organisms, a certain variance, v, was induced in the growth parameter μ. For each organism, a value of μ was

randomly selected from a log-normal distribution of μ values with mean $\bar{\mu}$ and variance v, as shown in the extract of MATLAB code below

```
pd = makedist('Lognormal','mu',log(E1^2/sqrt(v+E1^2)),
   'sigma',sqrt(log(v/E1^2+1)));
mu = random(pd);
```

where pd is a log-normal distribution of μ values and $E1 = \bar{\mu}$. Handled this way, the growth parameter was effectively a compartment in which the uncertainties in the rest of the parameters were incorporated. Had a constant growth parameter been adopted, all simulated organisms would produce identical results, suggesting zero uncertainty in all parameters.

Table 3 in Appendix A shows a collection of the parameter values that were used with the Wilkie model. The parameters α_{rad} and β_{rad} in equation 2.29 were assigned the values 0.02 Gy^{-1} and 0.002 Gy^{-2}, respectively, which were chosen as typical for cancer cells [6]. The values of r and θ in the absence of any kind of therapy were $1 \cdot 10^{-3}$ and 2.5, respectively. According to Wilkie and Hahnfeldt [7], the presence of an immunotherapy drug can be modelled by an increase in the immune recruitment factor r as well as the predation strength θ to the values $(r, \theta) = (0.47, 4)$. This suggests a non-specific immunotherapy mechanism, but is still useful for studying the synergy with radiotherapy. It has been established earlier that radiation induces antigen release in cancer cells. For that reason, the recruitment factor was adjusted to model radiation-induced immune-recruitment. The ratio of radiation-induced to intrinsic antigen release in tumours was taken to be 200 [6]. There was no consideration of a specific dose of immunotherapy; it was its presence that was of the essence. Simulations were run in the four cases of no treatment, treatment with immunotherapy alone, treatment with radiation alone and treatment with the combination of radiotherapy and immunotherapy. In actual experiments (with rats or mice), the organisms are terminated when the tumour reaches a size at which they show pronounced symptoms of cancer. The tumour is thus not left to grow to the carrying capacity. To mimic this effect, integration of equations 2.26 and 2.27 was ceased as soon as the tumour grew to a size corresponding to a mass of 100 mg. The outcomes of the treatments were evaluated by studying the lifetime of the simulated organism under each treatment modality. Different radiation dose schemes were attempted with the purpose of verifying a dependence of the efficacy of the combination therapy on fractionation. Conversion from tumour cell number (X) to tumour diameter in millimetres (d) was done by treating the tumour as a sphere and using that $1\text{mm}^3 = 10^6$cells [13]. Thus

$$d(X) = 2 \cdot \left(\frac{X}{10^6} \frac{3}{4\pi} \right)^{1/3} \tag{2.32}$$

For conversions between tumour diameter and mass, it was further assumed that the tumour is a water-containing sphere and thus the density of water was used.

2.2 Serre model

The Serre model was intrinsically designed to model the combination of radiotherapy and immunotherapy. It considers tumour-immune interaction via the release of tumour-associated antigens that trigger an anti-tumour immune response. The immune response is cleft into a primary and a secondary compartment.

2.2.1 Tumour evolution

The time evolution of the tumour mass is described by

$$T_{n+1} = S_n(d) \cdot T_n \cdot e^{\mu - Z_{prm,n} - Z_{sec,n}} \tag{2.33}$$

$T_i, i \in \mathbb{N}$, is the tumour mass on day i, given in grams. $S_n(d)$ is the survival probability of the tumour upon exposure to a radiation dose d on day n (as defined by equation 2.29). μ is a growth parameter such that, without any treatment, the tumour grows by e^{μ} each day. This is also assuming that there is no response from the immune system. $Z_{prm,n}$ and $Z_{sec,n}$ are the responses of the immune system (primary and secondary, respectively). The immune system can either slow down tumour growth ($Z_{prm,n} + Z_{sec,n} < \mu$) or reverse it altogether ($Z_{prm,n} + Z_{sec,n} > \mu$). Equation 2.33 is necessarily recursive since the tumour mass on a given day must depend on its value on the previous day.

2.2.2 Antigen population

Antigens are danger-associated molecules emitted by the tumour. The quantity of tumour antigens on a given day i, A_i, is given by

$$A_{n+1} = (1 - \lambda) \cdot A_n + \rho \cdot T_n + \psi \cdot (1 - S_n(d)) \cdot T_n \tag{2.34}$$

The non-irradiated tumour secretes antigens intrinsically at a constant rate ρ. As mentioned in section 1.3, radiation can give rise to the release of antigens in tumour cells. Assuming antigens are released only by dying tumour cells, their rate of release is necessarily proportional to the probability of death of the cells $(1 - S_n(d))$. ψ is a constant that represents radiation-induced tumour cell immunogenicity. $\lambda \in [0, 1]$ models the rate at which the tumour antigens recede, and are replaced by immune effector cells.

2.2.3 Lymphocyte population

The number of immune effector cells present at the tumour site on day i, L_i, is given by

$$L_{n+1} = (1 - \phi) \cdot \delta_n \cdot L_n + \lambda \cdot A_n \tag{2.35}$$

ϕ represents the constant rate at which the immune effector cells leave the system and δ_n is the probability that immune cells in the tumour survive irradiation on day n. λ is as defined earlier. The immune effector cell population depends on both the population of antigens and immune effector cells on the previous day.

2.2.4 Primary immune response

The primary immune response is described by

$$Z_{prm,n} = \frac{\omega \cdot L_n}{1 + \frac{\kappa \cdot T_n^{\frac{2}{3}} \cdot L_n}{1+p_1}} \tag{2.36}$$

$Z_{prm,n}$ is the primary immune response on day n. $1/[1 + \frac{\kappa \cdot T_n^{\frac{2}{3}} \cdot L_n}{1+p_1}]$ is the fraction of activated immune effector cells that are at work against the tumour. κ is a constant describing the ability of the tumour to naturally suppress an immune response while ω is a proportionality constant. p_1 represents the concentration of an immunotherapy drug that functions by inhibiting the expression of the PD-L1 ligand by the tumour. As was pointed out in section 1.2, the primary immune response is elicited by the immune effector cells and as such must depend on the population of these cells as equation 2.36 shows.

2.2.5 Secondary immune response

The secondary immune response is given by

$$Z_{sec,n} = \sum_{k=0}^{n} \gamma \cdot \frac{1 + c_4}{r + c_4} \cdot Z_{prm,k} \tag{2.37}$$

$Z_{sec,n}$ is the secondary immune response on day n. γ represents the likelihood of the primary immune response to trigger a secondary response, per time-step. c_4 represents the concentration of an anti-CTLA4 immunotherapy drug and r is a constant chosen to be larger than 1 so that, without an anti-CTLA4 drug, the likelihood of a secondary response is less than γ. The summation suggests that the secondary response is a cumulative effect that will only come to life after a certain time delay. It was mentioned in section 1.2 that the secondary immune response is a memory response and it occurs only after there has been a primary immune response (primary contact with the invading species). It thus depends directly on the primary response as equation 2.37 illustrates.

The essence of the Serre model is that radiation induces the secretion of tumour antigens that activate immune effector cells. Worth reiterating is that the tumour intrinsically emits antigens, but exposure to radiation increases their expression, quantity and variety [23]. The effector cells then stage a primary immune response against the tumour which gives rise to a secondary anti-tumour response. The anti-CTLA-4 medicine functions by enhancing the secondary immune response while anti-PD1 immunotherapy inhibits the immunomodulatory effect of the tumour.

2.2.6 Implementation

The Serre model was fitted to the experimental data of Ahlstedt et al. [20] and Ceberg et al. [24], using MATLAB's fminsearch fitting tool and the shooting method. The data

consisted of median survival times of cancer-affected organisms (glioblastoma- innoculated rats) under no treatment, treatment with only immunotherapy, only radiotherapy and with a combination of immunotherapy and radiation. Median survival time is to be interpreted in this context as the time at which exactly half of the treated organisms are still alive. Beyond this time, more than half of the organisms undergoing treatment have died.

It should be noted here that, although the Serre model describes the dynamics of a general tumour type, the experimental data used to deduce its parameters was obtained from breast tumours. The data of Ahlstedt et al. and Ceberg et al, however, was measured on brain tumours (glioblastoma). Although unclear how, this discrepancy potentially threatens the quality of the results since not all the parameters in the Serre model could be fitted to the available experimental data. It was assumed that such parameters as reflect the characteristics of the immune system, for instance, the propensity of the primary immune response to induce a secondary response, could be regarded as independent of either the position or type of the tumour. Furthermore, the Serre model was designed for combination of radiotherapy with specifically anti-PD-L1 and anti-CTLA4 immunotherapy. On the contrary, the data from Ahlstedt et al. was measured for the combination of radiotherapy with the anti-IDO drug, 1-MT. The model was modified to replace the anti-PD-L1 and anti-CTLA4 drugs with 1-MT. This was done by setting the values of the parameters p_1 and c_4 in equations 2.36 and 2.37 to zero. The action of 1-MT was then captured in the parameter ω in equation 2.36. In this respect, the inhibition of IDO was assumed to have a more robust effect than the inhition of the PD-L1 and CTLA4 pathways. The growth parameter μ was handled exactly the same way as was done with the Wilkie model, but with the mean $\bar{\mu}$ fitted to experimental data. During the fitting process, median survival times of the organisms were estimated by the Kaplan-Meier method [25]. In medical research, the Kaplan-Meier method is used to estimate the survival function (fraction of organisms alive after a certain time post-treatment). It is an estimator that, given the lifetimes of organisms in a group, computes the probability that a given number of the organisms were alive after a certain time [28].

As with the Wilkie model, simulations were carried out in the cases of no treatment, treatment with immunotherapy alone, radiotherapy alone and a combination of both. By studying median survival times, the optimum dose fractionation was deduced. Table 4 in Appendix B shows the values of parameters adapted from Serre et al. and those fitted to the data of Ahlstedt et al [20] and Ceberg et al. [24]. As with the Wilkie model, no consideration was made of a specific dose of 1-MT. The fitting process produced the value of ω in the presence of 1-MT, and this value was used throughout the investigation.

3 Results and Discussion

Findings obtained from simulations with both the Wilkie and Serre models are presented in this section. The results cover, for each model, the cases of no treatment, treatment with immunotherapy alone, radiation alone, immunotherapy with one 8 Gy radiation dose and with two such doses. The dependence of treatment efficacy (measured by median survival time) on dose fractionation (the spacing between the two 8 Gy doses) was also studied for both models.

3.1 Wilkie model

Figures 2 and 3 show the results generated with the Wilkie model for the case of no treatment. The purpose of these results was first to verify that the tumour progression followed the generalised logistic growth (sigmoid curve) of unperturbed tumours and, second, to compare with tumour evolution influenced by treatment. Figure 2 confirms the expected tumour growth, with an abrupt termination at a diameter corresponding to a tumour mass of 100 mg. This cutoff, as noted earlier, was imposed to resemble the elimination of organisms at a certain tumour mass to prevent excessive suffering in an *in vivo* experiment. The median survival time of the organisms was estimated using the Kaplan-Meier method [25] and a plot of the survival function is shown in Figure 3. The survival function is constantly unity until it drops abruptly to null, consistent with the tumour evolution shown in Figure 2.

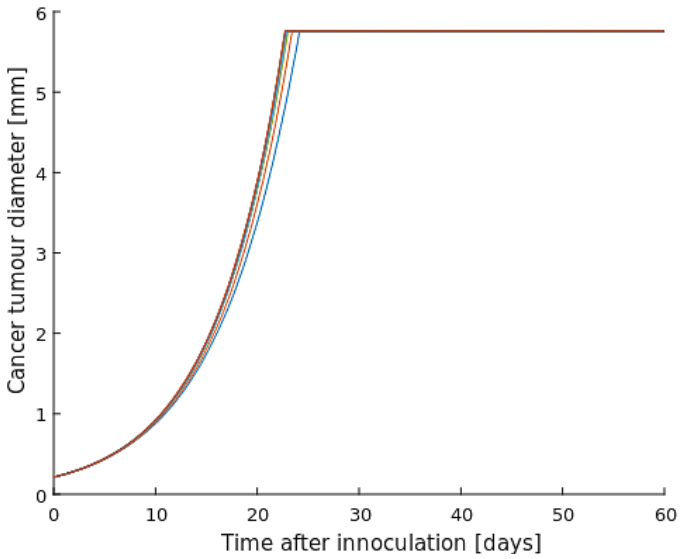

Figure 2: Tumour progression in nine organisms (rats) in the absence of treatment

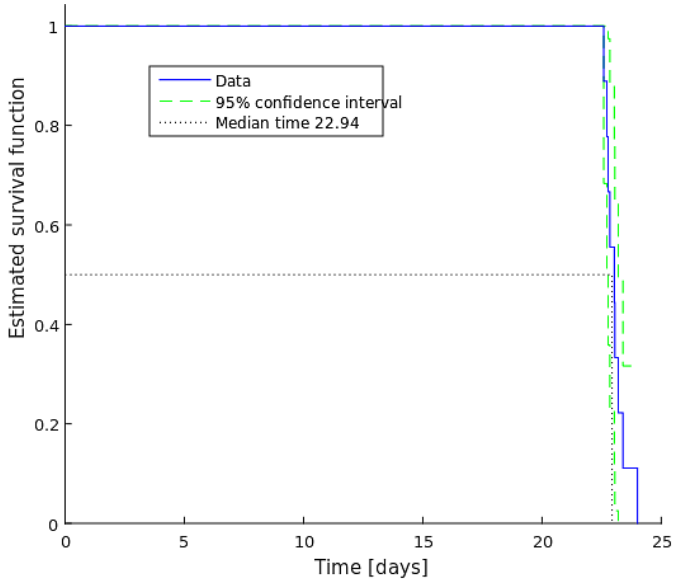

Figure 3: The survival function corresponding to the tumour development of Figure 2

3.1.1 Synergy

The Kaplan-Meier method [25] was used to obtain median lifetimes for the four treatment modalities involving single-dose radiation alone, immunotherapy alone and immunotherapy in combination with radiation given in both single- and double-dose fractionations. The results are shown in Table 1 below.

Table 1: Cancer treatment results generated with the Wilkie model

Therapy	Radiation dose [Gy]	Day given	Median lifetime [days]
radiotherapy	8	7	23.81
immunotherapy	-	7 to 80	22.93
radiation+ immunotherapy	8	7	24.11
radiation+ immunotherapy	8; 8	7 ; 15	25.25

Table 1 reflects a marginal increase in the median lifetime when immunotherapy is administered alone, compared to the 22.9-day median survival time observed in the absence of treatment. According to the theory discussed in section 1.2, that immunotherapy applied independently fails to reverse the process of immunoediting, this result is sound. Radiotherapy administered independently was observed to give rise to longer survival than immunotherapy did, a reasonable outcome given that radiation is not subject to cancer

immunoediting, but instead retards tumour growth by directly annihilating tumour cells. As is apparent from the table, there was an evident rise in survival time when immunotherapy was combined with a single radiation dose compared to the observed survival times with either therapy alone. This result was expected, as it coheres with the theory provided in section 1.3. Irradiation kills off a fraction of cancer cells and at the same time enhances immune recruitment through stimulating emission of tumour-associated antigens, giving rise to the observed synergy with immunotherapy. As is shown in Table 1, combining immunotherapy with two doses of radiation led to an even higher treatment efficacy, clearly suggesting a preference for the double-dose fractionation scheme.

3.1.2 Fractionation

The one-week interval between the two radiation doses shown in Table 1 is not trivial. Recalling the theory in section 1.3, the success of the combination of radiotherapy and immunotherapy hinges on the radiation dose fractionation. It was thus of interest to study how the treatment efficacy (median survival time) depends on fractionation (dose spacing) and Figure 4 shows the result. The figure reflects notably that the median survival time is indeed a function of dose fractionation. With the two radiation doses given on the same day, the resulting survival was observed to match that resulting from a single dose (median 24.11 days, Table 1). A constant, maximum median survival time of 25.25 days was observed for dose spacings ranging from 1 to 30 days. This is consistent with the value quoted in Table 1, which corresponds to a dose spacing of 7 days. Figure 4 shows a drastic decline in efficacy beyond the 30 day interval, settling to a constant, minimum median survival of 24.11 days. This result suggests that the importance of the second dose diminishes if it is delivered much later (later than 4 weeks) than the first dose. A possible explanation for this observation is that, even though the first dose kills off some tumour cells and instills antigen emission, its effect may be adequate to disrupt tumour immunoediting (and thus modulate tumour growth), but inadequate to reverse this process. The second dose then serves to broaden the pool of tumour-associated antigens, further disrupting and possibly halting immunoediting. As discussed in section 2.1, tumour advancement passes through a state of equilibrium that may, depending on the balance between tumour-regulatory and immunosuppressive responses, lead to either tumour elimination or escape. With this in mind, the second radiation dose (given early enough) will either lead to tumour elimination or tumour escape with a prolonged survival time for the organism. A second dose administered too late does not give rise to a noticeable effect compared to the single-dose case because at that stage, the tumour has passed the equilibrium phase and escaped.

Be that as it may, the resolution in Figure 4 is rather inferior. The observed step-function behaviour of the median survival time curve bears no resemblance to a physical situation. Furthermore, the difference between the maximum and minimum median survival times in the figure is merely 1 day, which would be insignificant were this model

applied to human patients. The inferiority of the results owes itself to the fact that there was no way of fitting the effect of irradiation to the experimental data of Tanooka et al. [27] used to estimate parameters in the Wilkie model. Had radiotherapy been used in the experiments by Tanooka et al. [27], it would have been possible to fit the constants of the linear-quadratic model to that data, incorporating the effect of radiation in a more comprehensive manner. Nonetheless, the results of simulations with this model still reflect clearly both a synergistic effect of combining radiotherapy with immunotherapy and a dependence of the success of this treatment modality on the radiation dose fractionation. This confirmation provided the opportunity for further, more focused study with the Serre model.

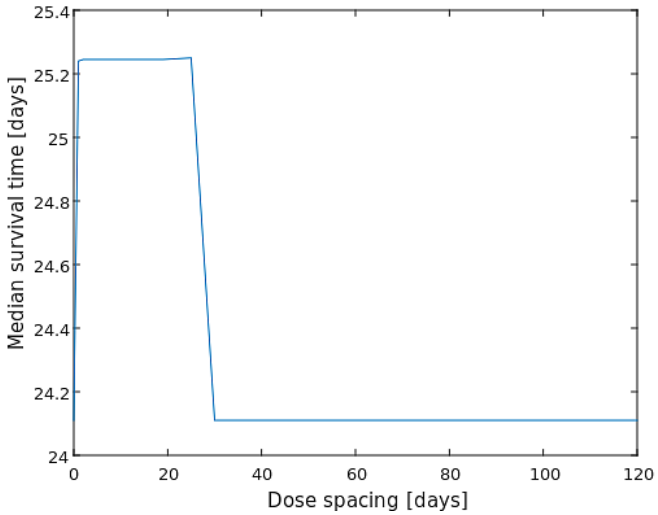

Figure 4: Variation of median survival time with radiation dose fractionation in combination therapy involving immunotherapy and radiotherapy

3.2 Serre model

Data for the untreated case, generated with the Serre model by fitting the growth parameter to the experimental data of Ahlstedt et al. [20] and Ceberg et al. [24], is shown in Figure 5. The results are analogous to those described in section 3.1, except that the Serre model was calibrated with experimental data prior to simulations. Figure 5 shows the typical logistic growth similar to the one shown in Figure 2. The data series plotted with red markers is experimental data for an untreated tumour obtained from Aas et al. [26]. This data was plotted as a reference. A Kaplan-Meier estimate of the survival function, similar to the one shown in Figure 3, was also generated for this case. The plot can be found in Appendix D.

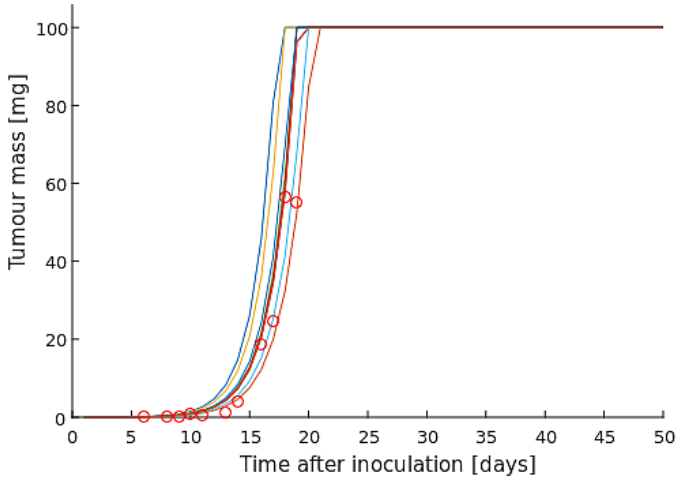

Figure 5: Tumour progression in nine organisms (rats) in the absence of treatment. The red markers show experimental data for an untreated tumour.

3.2.1 Synergy

In order to examine the coaction between radiotherapy and immunotherapy (1-MT), median survival times were computed for the exact same four treatment modalities considered with the Wilkie model. Table 2 below shows the results.

Table 2: Cancer treatment results generated with the Serre model

Therapy	Radiation dose [Gy]	Day given	Median lifetime [days]
radiotherapy	8	7	19.80
1-MT	-	7 to 50	19.50
radiation + 1-MT	8	7	28.75
radiation + 1-MT	8; 8	7 ; 15	35.75

With the administration of radiotherapy or immunotherapy independently, only a slight increase in median survival was observed, further confirming that these therapies are ineffective on their own. The effects of the two therapies are comparable, with radiation leading to marginally higher efficacy, cohering with what was observed with the Wilkie model. The general trend in the results in Table 2 matches that in Table 1, a compelling result considering that the two models were independent. However, contrary to the Wilkie model, the Serre model predicts a drastic rise in efficacy upon treatment with a combination of immunotherapy and single-dose radiation. This discrepancy could yet again have been caused by the incomprehensive way in which radiation was incorporated into the Wilkie model. Table 2 shows as even higher treatment efficacy with two

8 Gy radiation doses given alongside 1-MT, again verifying the higher potential in using a double-dose fractionation. Important to note, nonetheless, is that in this last case, the median survival time bears relatively less meaning because the treatment was in fact curative. Cancer tumours in the majority of organisms were eliminated and this is a key difference between the results of this model and those of the Wilkie model. In none of the cases in simulations with the Wilkie model was the tumour eliminated.

Consider Figure 6 which shows the time-evolution of the tumour in the case of immunotherapy with two 8 Gy radiation doses. The majority of the tumours shown are eliminated well before attaining the fatal mass of 100 mg.

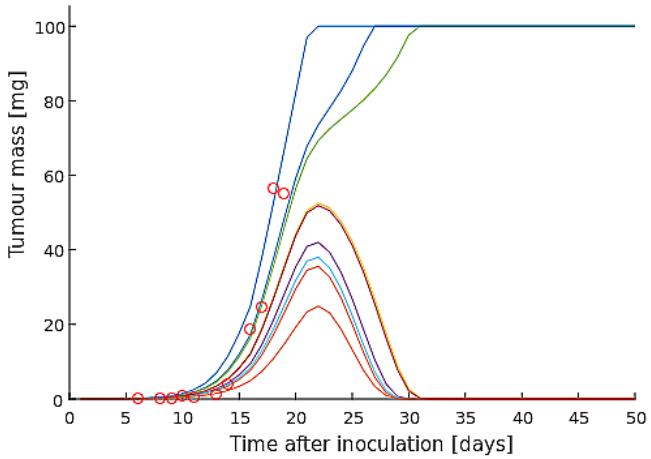

Figure 6: Tumour evolution in 9 rats treated with 1-MT and two 8 Gy radiation doses given on days 7 and 15 post-innoculation. The red markers show untreated tumour data.

3.2.2 Fractionation

The 7-day dose spacing chosen for the treatment in Figure 6 was selected primarily because simulations with the Wilkie model had shown it to lead to high treatment efficacy. However, a study of the dependence of efficacy on fractionation with the Serre model revealed that this dose-interval was in fact one of the optimum. As with the Wilkie model, Kaplan-Meier estimates of median survival times were obtained and plotted against the corresponding dose spacing. Figure 7 below presents the results. For those cases in which the treatment was curative, in all organisms, the patient group was assigned a median survival time of 50 days. The figure shows a relatively low treatment efficacy when the two doses are given on the same day (that is, a single dose of 16 Gy given on day 7). This supports the choice of a fractionation scheme involving two separate doses instead. Between days 1 and 8, a constant, maximum efficacy was observed, in which the treatment was invariably curative. Beyond the 8 day interval, the treatment efficacy declines drastically, thereafter gently approaching that observed with a single dose of 8 Gy in combination

with 1-MT. The general trend of these results bears irrefutable resemblance to that of the results in Figure 4. As for the actual values of the dose spacing, it is the results of the Serre model that have the higher credibility, owing to the fact that this model was rigorously adapted to the experimental data of Ahlstedt et al. [20] and Ceberg et al [24].

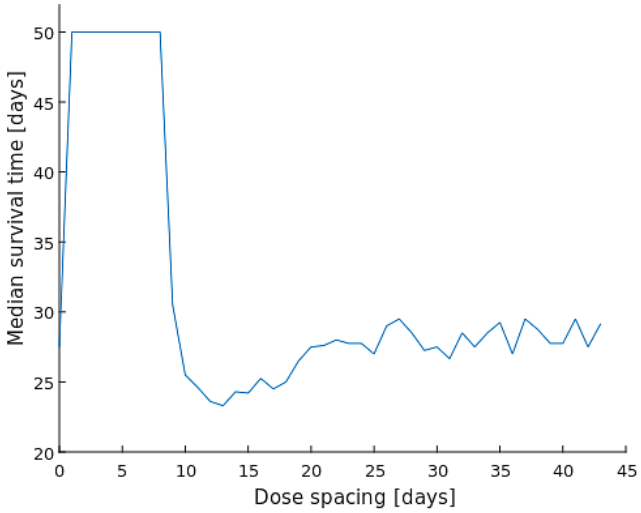

Figure 7: Variation of median survival time with fractionation in the combination of 1-MT and two 8 Gy radiation doses. 50-day median survival times indicate curative treatment.

4 Outlook

In a word, this thesis work has been successful in realising its objective of verifying the existence of a synergy between radiotherapy and immunotherapy and, more importantly, determining the optimum radiation dose fractionation that ensures the highest treatment efficacy. The results from simulations with the Wilkie model and, more importantly, the Serre model, provide compelling support for the success of the treatment modality combining immunotherapy (in particular, 1-MT) with two 8 Gy doses of radiation given no more than a week apart. Promising is the fact that the two models employed in this work exhibited a level of consensus on this result, despite that they were independently derived. Nevertheless, in deducing both models used in this work, numerous assumptions were made about the immune system and its interaction with a cancer tumour. These assumptions may cause the results of simulations with these models to deviate significantly from clinical or experimental results. Until confirmed by either experimental or clinical trials, deductions from computer simulations can not be celebrated.The outcome of this work is to be interpreted as forming a hypothesis - a foundation upon which either further *in silico* research or *in vivo* experiments can be built.

References

[1] Stewart BW, Wild CP.World Cancer Report 2014. International Agency for Research on Cancer. World Health Organization. 2014

[2] Soukup K, Wang X. Radiation meets immunotherapy - a perfect match in an era of combination therapy?. Int J Radiat Biol. 2015; 91(4):299-305

[3] Swapan KR. Glioblastoma, Molecular Mechanisms of Pathogenesis and Current Therapeutic Strategies. New York: Springer Science + Business Media,LLC; 2010

[4] Gandhi SJ, Minn A, Vonderheide RH, Wherry EJ, Hahn SM, Maity A. Awakening the immune system with radiation: Optimal dose and fractionation. Cancer Lett. 2015; 368(2):185-90

[5] Schuster M, Nenchansky A, Ralf K. Cancer immunotherapy.Biotechnol J. 2006; 1(2):138-47

[6] Serre R et al. Mathematical Modeling of Cancer Immunotherapy and Its Synergy with Radiotherapy. Cancer Res. 2016; 76(17):4931-40

[7] Wilkie KP, Hahnfeldt P. Tumour-Immune Dynamics Regulated in the Microenvironment Inform the Transient Nature of Immune-Induced Tumour Dormancy. Cancer Res. 2013; 73(12):35344-44

[8] Han W, Yu KN. Response of cells to ionising radiation. Bentham Science Publishers Ltd. 2009

[9] Jeffrey Coderre. 22.55J Principles of Radiation Interactions. Fall 2004. Massachusetts Institute of Technology: MIT OpenCourseWare, https://ocw.mit.edu. License: Creative Commons BY-NC-SA.

[10] The Internation Commission on Radiation Units and Measurements. Fundamental quantities and units for ionising radiation (revised). Journal of the ICRU. 2011; 11(1):85

[11] Satow T, Kawai Hajime. Hit and Target Models for DNA Damage with Indirect Action. Computers and Mathematics with Applications. 2006; 51:257-268

[12] McBride B. The Radiobiology Behind Dose Fractionation. Dept. Radiation Oncology, David Geffen School of Medicine. UCLA, Los Angeles. 2009

[13] Benzekry S et al. Classical Mathematical Models for Description and Prediction of Experimental Tumour Growth. Growth. PLos. Comput. Biol. 2014; 10(8):e1003800

[14] Mombach J, Lemke N, Bodmann B, Idiart. A mean-field theory of cellular growth. Eur Lett. 2002; 59: 923–928

[15] Wilson S, Grenier E, Wei M, Calvez V, You B, et al. Modeling the synergism between the anti-angiogenic drug sunitinib and irinotecan in xenografted mice. 2013; PAGE 22. p. 2826.

[16] Baskar R, Lee KA, Yeo R, Yeoh K. Cancer and Radiation Therapy: Current Advances and Future Directions. Int. J. Med. Sci. 2012; 9(3):193-199

[17] Brenner DJ. The Linear-Quadratic Model Is an Appropriate Methodology for Determining Isoeffective Doses at Large Doses Per Fraction. Semin. Rad. Oncol. 2008; 18:234-239

[18] Jeanbart L, Swartz MA. Engineering opportunities in cancer immunotherapy. Proc. Natl. Acad. Sci. USA. 2015; 112(47):14467-72

[19] Buchbinder EI, Desai A. CTLA-4 and PD-1 Pathways - Similarities, Differences, and Implications of Their Inhibition. Am. J. Clin. Oncol. 2016; 39(1):98-106

[20] Ahlstedt J, Förnvik K, Ceberg C, Nittby HR. Effect of Blockade of Indoleamine 2,3-dioxygenase in Conjuction with Single Fraction Irradiation in Rat Glioma. JJ. Rad. Oncol. 2015; 2(3):022

[21] Ceberg C, Persson BRR. Co-operative radio-immune-stimulating cancer therapy. Medical Radiation Physics, Lund University. 2013

[22] Demari S. Golden EB, Formenti SC. Role of Local Radiation Therapy in Cancer Immunotherapy. JAMA Oncol. 2015; 1(9):1325-32

[23] Kalbasi A, June CH, Haas N, Vapiwala N. Radiation and immunotherapy: a synergistic combination. J. clin. Invest. 2013; 123(7):2756-63

[24] Ceberg C et al. Photon activation therapy of RG2 glioma carrying Fischer rats using stable thallium and monochromatic synchrotron radiation. Phys. Med. Biol. 2012; 57(2012):8377-8391

[25] Cardillo G. KMPLOT: Kaplan-Meier estimation of the survival function. 2008

[26] Aas AT, Brun A, Blennow C, Strömblad S, Salford LG. The RG2 rat glioma model. Journal of Neuro-Oncology. 1995; 23:175-183

[27] Tanooka H, Tanaka K, Arimoto H. Dose response and growth rates of subcutaneous tumors induced with 3-methylcholanthrene in mice and timing of tumor origin. Cancer Res. 1982; 42:4740–4743

[28] Goel MK, Khanna P, Kishore J. Understanding survival analysis: Kaplan-Meier estimate. Int J Ayurveda Res. 2010; 1(4):274-278

Appendix

A

This appendix contains the parameter values that were used in simulations with the Wilkie model, shown in Table 3 below.

Table 3: Parameter values used with the Wilkie model

Parameter	Value	Unit	Meaning
$\bar{\mu}$	0.16	day^{-1}	cancer growth
α	0.72	none	cancer growth
λ	0.22	day^{-1}	immune growth
r	$1 \cdot 10^{-3}$	none	immune recruitment
θ	2.5	none	predation strength
β	0.5	none	predation saturation
ϕ	50	none	predation saturation
ϵ	0.01	none	innate immunity predation strength
K_C	$3.92 \cdot 10^{10}$	cell number	cancer carrying capacity
K_I	$3.92 \cdot 10^{10}$	cell number	immune carrying capacity
C_{max}	$1 \cdot 10^{8}$	cell number	maximum permitted tumour population

Appendix

B

This appendix contains the parameter values that were used in simulations with the Serre model, presented in Table 4 below.

Table 4: Parameter values used with the Serre model

Parameter	Value	Unit	Meaning
Fitted to experimental data			
$\bar{\mu}$	0.576	none	daily cancer growth parameter
α_{rad}	0.0475	Gy^{-1}	linear radiosensitivity of tumour cells
β_{rad}	0.00475	Gy^{-2}	quadratic radiosensitivity
ω_n	0.044	none	primary immune response strength
Assumed invariant under change of tumour type			
ω	0.007	none	primary immune resposne sensitivity
p_1	0	none	anti-PD-L1 drug concentration
c_4	0	none	anti-CTLA4 drug concentration
ρ	0.1	none	intrinsic tumour antigen release
ψ	20	none	radiation-induced antigen release
γ	0.03	none	secondary immune resposne probability
r	5	none	dimensionless constant
λ	0.15	none	tumour antigen disappearance
ϕ	0.1	none	daily disappearance of immune effectors
κ	0.01	none	primary immmune response sensitivity
C_{max}	100	mg	maximum permitted tumour mass

Appendix

C

This appendix contains the MATLAB code that was used in the implementation of the Wilkie model. The code uses a 4th order Runge-Kutta method to numerically solve the two differential equations in the Wilkie model. It consists of the main script entitled "IMPLEMENTATION OF THE WILKIE MODEL USING A 4TH ORDER RUNGE-KUTTA ROUTINE" and five functions named "radiation", "immune", "cancer, "predation" and "convertor". The comments in the code describe explicitly what each part of the code does.

```
%IMPLEMENTATION OF THE WILKIE MODEL USING A 4TH ORDER RUNGE-KUTTA ROUTINE
%http://mathworld.wolfram.com/Runge-KuttaMethod.html
%http://lpsa.swarthmore.edu/NumInt/NumIntFourth.html
%%
clear all;
close all;
%clf(1);
%These are the equations we will use:
% C'(t) = (mu/alpha)*(1 + psi)*C*(1 - ((C/Kc)^alpha)) = cancer(C(n), psi(n), mu);
%immune population (cell number)
% psi = -theta*(((I^beta)/(phi*(C^beta) + (I^beta)))  +  epsilon*log10(1 + I)) =
%predation(I(n), C(n), theta(n)); %immune predation
% I'(t) = lambda*(1 + rC)(1 - (I/Ki)) = immune(I(n), C(n), r(n));
%cancer population (cell number)
%%
%initialising arrays
Q = 9;
t_stop = 120;        %120 days,the time for which the patients are followed
N = 12000;          %number of iterations; 100 iterations per day
dt = t_stop/N;      %time-step
t(1) = 0;           %initialising the time-array
C(1:Q) = 5000; %initial number of tumour cells
I(1:Q) = 0; %no immune presence at time of detection
psi(1) = 0; %no immune predation at time of detection
Cmax = 1E8; %terminate patient when the tumour reaches this size (1E8 cells = 100mg)

%radiation
d(1:N) = 0;
for h = 651:654
```

```
d(h) = 18/4; %this is equivalent to d(7) = 8, just done in 100 steps.
end
for k = 2951:2954
d(k) = 18/4; %this is equivalent to d(15) = 8, just done in 100 steps.
end

%immune predation strength
theta(1:N) = 2.5; %adjust this to model an immune therapy medicine. 2.5 is the
%no-treatment value from Wilkie
%and 4 is the with-treatment value
for h1 = 601:80000
theta(h1) = 4; %begin immune therapy on day 7; going beyond day 80 is useless,
%the patients are most likely dead
end

%immune recruitment factor
r(1:N) = 1E-3; %adjust this to model an immune therapy medicine. 1E-3 is the
%no-treatment value from Wilkie and 0.47 is the with-treatment value
for k1 = 601:80000
r(k1) = 200; %begin immune therapy on day 7; no need to go beyond day 80
end

%Tumour growth parameter
E1=0.16; %Exponential tumour growth - mean %initial guess
% v=0.001; %Exponential tumour growth - variance
% pd=makedist('Lognormal','mu',log(E1^2/sqrt(v+E1^2)),'sigma',sqrt(log(v/E1^2+1)));
%Exponential tumour growth - log-normal distriution assumed


%%
%The RK4 routine
for q = 1:Q
C(q,1) = 5000;
I(q,1) = 0;
for n = 1:N-1
t(n+1) = t(n) + dt; %progress in time
psi(n+1) = predation(I(n), C(n), theta(n)); %get immune predation
mu = random(pd); %random mu value from distribution
%RK4 factors for the tumour (the method uses slopes to estimate values of tumour
%cell population)
```

```
c1 = dt*cancer(C(q,n), psi(n),mu);
c2 = dt*cancer(C(q,n)+ 0.5*c1, psi(n),mu);
c3 = dt*cancer(C(q,n) + 0.5*c2, psi(n),mu);
c4 = dt*cancer(C(q,n) + c3, psi(n),mu);
%RK4 factors for the immune system
i1 = dt*immune(I(q,n), C(q,n), r(n));
i2 = dt*immune(I(q,n) + 0.5*i1, C(q,n), r(n));
i3 = dt*immune(I(q,n) + 0.5*i2, C(q,n), r(n));
i4 = dt*immune(I(q,n) + i3, C(q,n), r(n));
%computing values of tumour cell population (the effect of radiation is included via
%the prefactor radiation(d(n)))
C(q,n+1) = min(Cmax, radiation(d(n))*(C(q,n) + (1/6)*(c1 + 2*c2 + 2*c3 + c4)));
%computing values of immune cell population
delta(n) = 1 - sign(d(n));
I(q,n+1) = delta(n)*(I(q,n) + (1/6)*(i1 + 2*i2 + 2*i3 + i4));
end
end
%%
%Longevity under treatment
for q = 1:Q
ttd=find(C(q,1:N)==Cmax,1,'first'); %calculate time to death (lifetime)
end
disp(['Patient died after ',num2str(t(ttd)),' days']) %report the lifetime

%a set of raw data for an untreated tumour, will be used to check if our
%simulations follow the  same trend for the untreated case
%        meas=[
% 6 2.69645E-05
% 8 0.000126337
% 9 0.000338363
% 10 0.000852692
% 11 0.000520944
% 13 0.001065318
% 14 0.003995114
% 16 0.018575225
% 17 0.024574458
% 18 0.056424422
% 19 0.0550847
% 20 0.03682267
% 21 0.029071125
```

```
% 22 0.044194261
% 23 0.035919072
% 24 0.077644006
% 25 0.11690166
% ];

%%
%Plotting
% figure (1)
% hold on
% for q = 1:Q
% C1(q,1:N) = convertor(C(q,1:N)); %convert the tumour size from cell number to
%diameter in mm
% plot(t(1:N),C1(q,1:N))
% xlabel('Time after innoculation [days]')
% ylabel('Cancer tumour diameter [mm]')
% end
MT = kmplot2(t(ttd))
% figure (2)
% kmplot(t(ttd))
%plot(meas(:,1),2*((((3000.*meas(:,2)./(4*pi)))).^(1/3)),'ro'); %plot the measured
%data as tumour diameter in mm against number of days
%%%%%%%%%%%%%%%%%%%%%%%%%%%%%%%%%%%%%%%%%%%%%%%%%%%%%%%%%%%%
```

Functions

```
function rad = radiation(d)
rad_alpha = 0.05; %the alpha constant for the linear-quadratic model
rad_beta = rad_alpha/10; %corresponding beta constant
%the above values have been chosen as typical values.

%this function returns the survival fraction of the tumour cells upon
%irradiation
rad = exp(-rad_alpha*d - rad_beta*d*d);
end

function i = immune(I, C, r)
%These are the values of parameters obtained from Wilkie and Hahnfeldt:
lambda = 0.22; %per day, immune growth
Ki = 3.92E10; %cell number, immune carrying capacity
%function returns the slope of the immune-population/time curve
```

```
i = lambda*(1 + r*C)*(1 - (I/Ki));
end

function c = cancer(C, psi, mu)
%These are the values of parameters obtained from Wilkie and Hahnfeldt:
alpha = 0.72; %cancer growth
%mu = 0.16; % cancer growth parameter (1 times the Wilkie value) (chosen to fit the
%untreated tumour data. The
%real significance of this was to calibrate the time scale, so
%that a time unit in this implentation would correspond to an actual day in
%the measured data)
Kc = 3.92E10; %cell number, cancer carrying capacity
%function returns the slope of the tumour-size/time curve
c = (mu/alpha)*(1 + psi)*C*(1 - ((C/Kc)^alpha));
end

function p = predation(I, C, theta)
%These are the values of parameters obtained from Wilkie and Hahnfeldt:
beta = 0.5; %predation saturation
phi = 50; %predation saturation
epsilon = 0.01; %innate immunity predation strength
%function returns the immune predation
p = -theta*(((I^beta)/(phi*(C^beta) + (I^beta)))  +  epsilon*log10(1 + I));
end

function conv = convertor(X)
%this function converts the tumour size from "number of cells" to "diameter in mm"
conv = 2*(((3.*X)/(pi*4E6)).^(1/3)); %conversion formula from Wilkie and Hahnfeldt
end
```

Appendix

D

This appendix contains the Kaplan-Meier estimate of the survival function in the case of an untreated tumour, simulated using the Serre model.

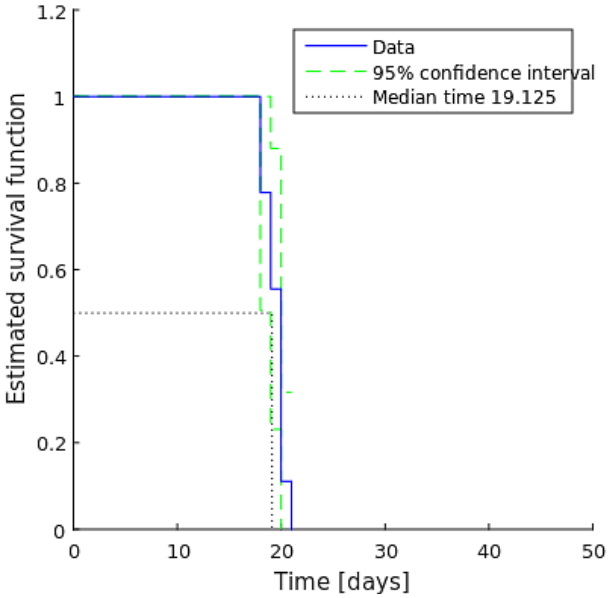

Figure 8: Kaplan-Meier estimate of the survival function corresponding to tumour progression in the absence of treatment. This figure was generated using the Serre model.

The survival function is constantly unity until it starts declining between days 15 and 20 where all the organisms perish with a median survival time of 19.1 days. This reflects exactly the tumour development shown in Figure 5.